

# Monster shocks, gamma-ray bursts and black hole quasi-normal modes from neutron-star collapse

Elias R. Most,<sup>1,2</sup> Andrei M. Beloborodov,<sup>3,4</sup> and Bart Ripperda<sup>5,6,7,8,9</sup>

<sup>1</sup>TAPIR, Mailcode 350-17, California Institute of Technology, Pasadena, CA 91125, USA

<sup>2</sup>Walter Burke Institute for Theoretical Physics, California Institute of Technology, Pasadena, CA 91125, USA

<sup>3</sup>Physics Department and Columbia Astrophysics Laboratory,

Columbia University, 538 West 120th Street New York, NY 10027, USA

<sup>4</sup>Max Planck Institute for Astrophysics, Karl-Schwarzschild-Str. 1, 85741 Garching, Germany

<sup>5</sup>Canadian Institute for Theoretical Astrophysics, 60 St. George St, Toronto, Ontario M5S 3H8

<sup>6</sup>Department of Physics, University of Toronto, 60 St. George St, Toronto, ON M5S 1A7

<sup>7</sup>David A. Dunlap Department of Astronomy, University of Toronto, 50 St. George St, Toronto, ON M5S 3H4

<sup>8</sup>Perimeter Institute for Theoretical Physics, 31 Caroline St. North, Waterloo, ON, Canada N2L 2Y5

<sup>9</sup>Center for Computational Astrophysics, Flatiron Institute, 162 5th Ave, New York, NY, 10010, USA

We perform the first magnetohydrodynamic simulation tracking the magnetosphere of a collapsing magnetar. The collapse is expected for massive rotating magnetars formed in merger events, and it may occur many hours after the merger. The results suggest a novel gamma-ray burst (GRB) scenario, which creates a delayed high-energy counterpart of the merger gravitational waves. The collapse launches an outgoing magnetospheric shock, and a hot magnetized outflow forms behind the shock. The outflow is modulated by the ring-down of the nascent black hole, imprinting its kilohertz quasi-normal modes on the GRB tail.

*Introduction.* Neutron star mergers are not only sources of gravitational waves, but are also accompanied by electromagnetic counterparts. Such counterparts provide insights into properties of dense matter in neutron stars and their magnetic fields. Canonical counterparts include a prompt gamma-ray burst (GRB [1]) and a kilonova ([2, 3]). Both were observed from the neutron star merger GW170817 (see, e.g., [4] for a summary). The GRB followed the merger with a 2-s delay and was likely emitted by a blast wave breaking out at the photosphere of the merger ejecta [5–8]. The kilonova was emitted on a day timescale and powered by nuclear decay in the expanding ejecta.

The explosion picture usually includes collimated relativistic jets from the black hole promptly formed after the merger. The jets are extremely bright sources of gamma-rays if observed face-on, and also emit a broad-band afterglow when they decelerate in an ambient medium [6]. However, some mergers may not promptly form a black hole and jets. Instead, they may form a long-lived neutron-star remnant [9, 10]. Its initial differential rotation is expected to generate magnetic fields up to  $B = 10^{16}$  G, which buoyantly emerge from the remnant and form its external magnetosphere [11–18]. Then, the remnant cools and forms a young magnetar. It likely has a twisted magnetosphere, filled with  $e^\pm$  pairs of a small mass density  $\rho$ . Its expected magnetization parameter  $\sigma = B^2 / (4\pi\rho c^2)$  is huge, exceeding  $10^{10}$  [19].

Eventually the remnant emits its angular momentum in a magnetized wind, loses its rotational support, and can collapse into a black hole [20–22]. The spindown occurs on the timescale  $t_{\text{sd}} \approx c^3 I / \mu^2 \Omega^2 \approx 10^4 \mu_{33}^{-2} (\nu / 300 \text{ Hz})^{-2}$  s, where  $I \approx 10^{45} \text{ g cm}^2$  is remnant’s moment of inertia,  $\nu = \Omega / 2\pi$  is its rotation rate and  $\mu$  is the dipole moment of its magnetosphere (we normalized it to  $10^{33} \text{ G cm}^3$ ). The delayed collapse after  $t \sim t_{\text{sd}}$  occurs suddenly, on a ms timescale.

Previous simulations of neutron-star collapse followed the dynamics of the external magnetosphere either in vacuum or

using force-free electrodynamics (FFE) [23–25]. Both frameworks do not allow plasma heating. Furthermore, both neglect plasma inertia and so are unable to track shock formation. By contrast, a full magnetohydrodynamic analysis predicts monster shocks, which can generate gamma-rays [19].

This Letter reports the first magnetohydrodynamic simulations of the magnetosphere evolution in the dynamic space-time of the collapsing star. It demonstrates shocks and ejection of a hot outflow that will emit a GRB. We also find that the outflow carries information about quasi-normal modes of the nascent black hole, which may be observed in the GRB time profile.

*Methods.* We set up a simple initial state: a dipole magnetic field is attached to a rotating star with  $\mu \parallel \Omega$ . We artificially reduce the rotation rate from a realistic  $\nu \gtrsim 300$  Hz to 56 Hz, so that the light cylinder  $R_{\text{LC}} = c/\Omega$  is beyond our computational box. This simplification avoids the challenging preparation of an equilibrium rotating magnetosphere with the equatorial current sheet at  $r > R_{\text{RL}}$ . Rotation is still essential, as it enables the ring-down effect when the star collapses into a black hole (e.g. [26]). The amplitude of ring-down oscillations scales with angular momentum. Therefore, we also simulate collapse with a high initial  $\nu = 900$  Hz; this additional simulation misses details of the outer magnetospheric dynamics but demonstrates the enhanced ring-down effect on the magnetized outflow from the nascent black hole.

The star is initialized as an unstable general relativistic polytrope of mass  $M = 1.7M_\odot$  and radius  $R_\star \approx 12$  km using the RNS code [27]; the details of its internal structure are unimportant, as we focus on the external magnetosphere. The magnetosphere has a low mass density  $\rho$  and a large magnetization parameter  $\sigma \gg 1$ . At time  $t = 0$ , we add a small pressure perturbation and the star begins to collapse.

The simulation tracks the spacetime of the collapsing star, and evolves its magnetosphere according to general relativistic magnetohydrodynamics (GRMHD) equations [28].

We use the Frankfurt/IllinoisGRMHD (FIL) code [29, 30] which is built on top of the Einstein Toolkit infrastructure [31]. The spacetime dynamics is tracked using the Z4c formulation of the Einstein equations [32]. We use moving puncture coordinates [33] in the simulation and the presentation of results below. The GRMHD equations assume an ideal fluid with thermal pressure proportional to  $e - \rho c^2$ , where  $e$  is the fluid energy density including rest mass. The equations are evolved using the ECHO scheme [34] with vector potential-based constraint transport [35, 36]. We employ a fixed three-dimensional Cartesian grid with 6 levels of mesh refinement; the highest resolution has 78 grid points per  $R_*$ , and extend to  $3.25 \times R_*$  in each direction.

Unlike previous MHD simulations in dynamical spacetimes (e.g. [29, 37–40]), our simulation follows the magnetosphere with a high magnetization parameter. In particular, the initial “background” magnetosphere has  $\sigma_{\text{bg}} \sim 25$ , and its perturbation during the collapse leads to ultra-relativistic motions with Lorentz factors  $\gamma \sim 10$ . Such simulations are challenging in terms of accuracy requirements and numerical stability of the algorithm, especially when MHD is coupled to a dynamically evolved spacetime. We have changed the code to improve its robustness (see also [41]), including different primitive recovery schemes [42, 43], drift floors [44], and bounds on  $\sigma$  and  $\beta = 8\pi P/B^2$  where  $P$  is the fluid pressure and  $B$  is the magnetic field in fluid rest frame. Even with all these improvements, we have found that the fourth-order derivative corrector performs poorly in the shock region. Since the constraint-transport algorithm prevents us from switching it off selectively, we have disabled it everywhere. Thus, the simulation maintains second-order accuracy, different from all previous GRMHD simulations carried out with FIL [12, 29, 41, 45, 46].

The evolution observed in the simulation may be summarized as follows.

*Collapse and wave launching.* The collapsing star quickly forms a black hole with horizon radius  $R_h \approx 2.5$  km and the ergosphere around it. Effectively, the magnetospheric footprints on the star are quickly pulled in from  $R_*$  to  $R_h$ , and the star’s magnetic flux  $\Psi$  is now threading the smaller sphere of radius  $R_h$ . As a result, a strong quasi-monopolar magnetic field  $B \sim \Psi/r^2$  is created in the radial zone  $R_h < r < R_*$ . This inner zone with the amplified magnetic pressure launches a compressive wave into the surrounding magnetosphere, which propagates with nearly speed of light,  $v_{\text{wave}}/c \approx 1 - \sigma_{\text{bg}}^{-1}$ .

The compressive MHD waves (known as “fast magnetosonic modes”) have electric field  $\mathbf{E} \parallel \mathbf{k} \times \mathbf{B}_{\text{bg}}$  where  $\mathbf{k}$  is the (approximately radial) wavevector and  $\mathbf{B}_{\text{bg}}$  is the initial background dipole magnetic field. So, the wave has a toroidal electric field  $E^\phi$ . The launched wave of  $E^\phi$  continues to propagate outward for the rest of the simulation; its snapshot is shown in Figure 1 at a late time  $t = 0.67$  ms (as measured by a distant observer), near the end of the simulation. The magnetic field ahead of the wave is the dipole  $\mathbf{B}_{\text{bg}}$ , and the magnetic field behind the wave is close to the split

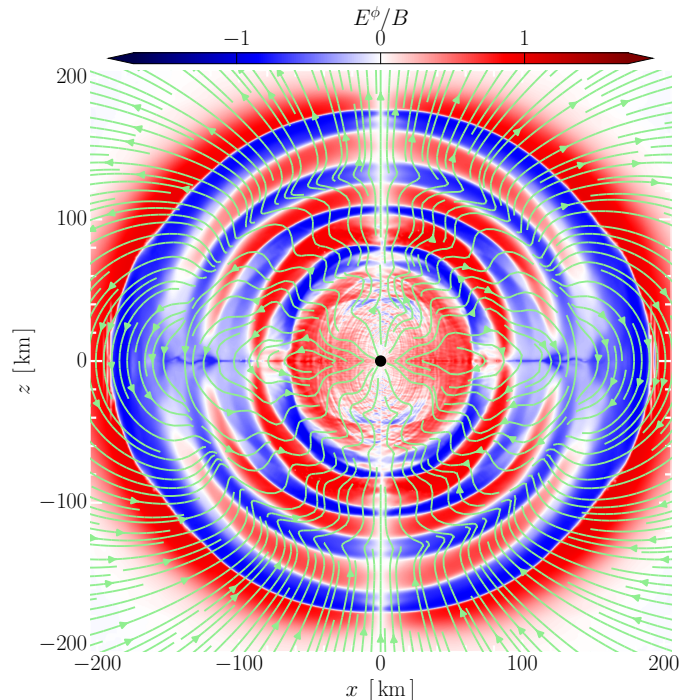


FIG. 1. Magnetohydrodynamic waves excited in the neutron star magnetosphere by the collapse. The rotation axis is along  $z$ , and the figure shows a cut of the magnetosphere along the plane of  $y = 0$ . The black circle at the center is the nascent black hole. Green curves show the magnetic field lines, and color shows  $E^\phi/B$  as measured by the local normal observer. The snapshot is taken at  $t = 0.67$  ms from the onset of collapse.

monopole configuration. The wave dynamics at radii  $r \gg R_h$  can be approximately described neglecting general-relativistic corrections.

*Monster shock formation.* Magnetosonic waves were recently shown to accelerate plasma to a huge radial 4-velocity  $u^r = \gamma v^r/c$  [19]. This effect occurs when the wave reaches radius  $R_\times = (c\mu^2/8L)^{1/4}$  in the equatorial plane, where  $\mu = r^3 B_{\text{bg}}$  and  $L$  is the wave power. In the FFE limit ( $\sigma_{\text{bg}} \rightarrow \infty$ ) fluid expansion in the rarefaction phase of the compressive wave would diverge at  $R_\times$  as  $E^2 - B^2$  touches zero and  $u^r \rightarrow -\infty$ . For a finite  $\sigma_{\text{bg}}$ , fluid develops a finite  $u^r \propto \sigma_{\text{bg}}$ . The ultrarelativistic fluid motion is directed toward the star and the wave immediately develops a monster shock.

Shock formation in magnetosonic waves has been demonstrated by kinetic plasma simulations [47] and by MHD calculations using characteristics [19]. For waves with frequency  $\omega \gg c/R_\times$  a simple analytical MHD solution has been obtained. It demonstrates that at  $r > R_\times$  the wave profile  $E(t - r/c)$  develops a plateau of width  $W_p \sim c/\omega$  where  $E^2 \approx B^2$ . The plateau forms a linear accelerator, so the wave pushes the fluid 4-velocity to a huge value [19]

$$u^r \approx -\frac{W_p \sigma_{\text{bg}}}{r} \approx -\frac{c \sigma_{\text{bg}}}{\omega r}. \quad (1)$$

The accelerated flow dissipates its energy in a monster shock.

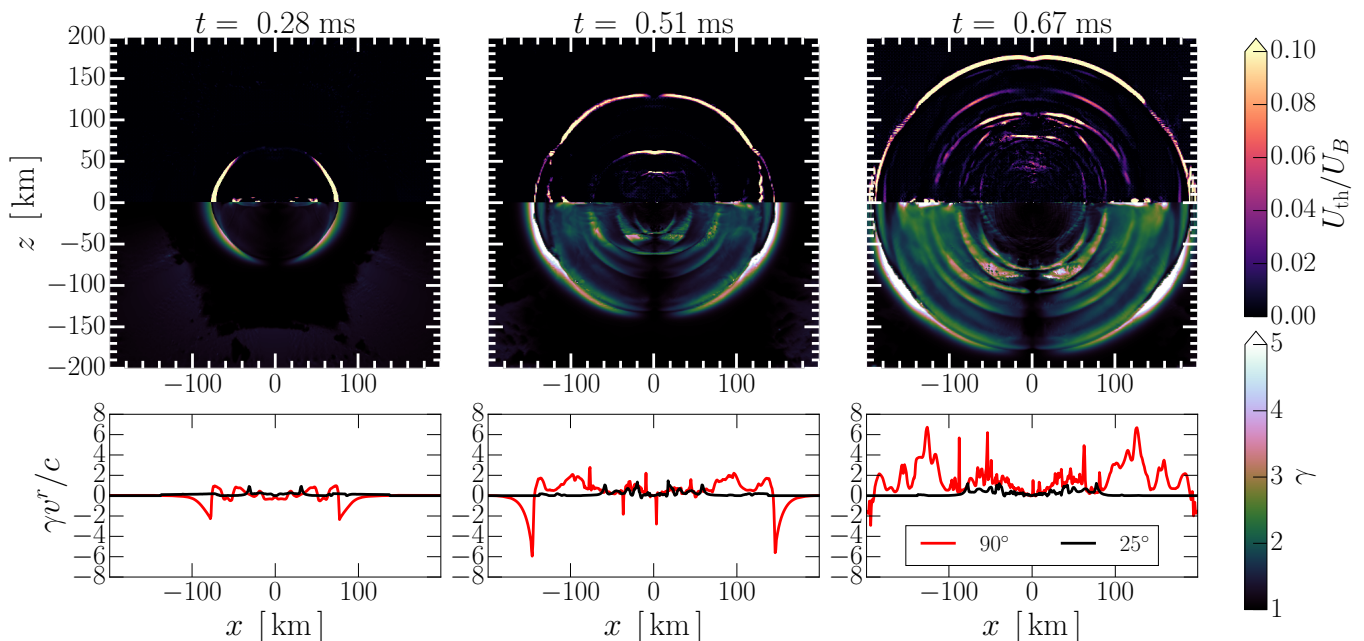


FIG. 2. Shock formation and evolution, shown with three snapshots (cuts of the magnetosphere along the vertical plane of  $y = 0$ ). Color panels show thermal energy density  $U_{\text{th}}$  (normalized to the magnetic energy density  $U_B$ ) at  $z > 0$  and fluid Lorentz factor  $\gamma$  at  $z < 0$ . Lower panels show the radial four-velocity  $u^r = \gamma v^r / c$  measured along two lines in the  $x$ - $z$  plane: on the  $x$ -axis (polar angle  $\theta = 90^\circ$ , red) and on the line of  $\theta = 25^\circ$  (black).

The monster shock appears in our simulation where  $E^2 - B^2$  approaches zero, as predicted. We also observe the development of an  $E$ -plateau where  $u^r$  develops a steep linear profile, reaching values consistent with Eq. (1) (see Fig. 2). The shock is the sudden jump of  $u^r$  from a large negative value  $u^r \sim -6$  back to a moderate  $u^r$ . These unique features of monster shocks are clear in the simulation despite numerical inaccuracies accumulated in the shock region. We also observe the expected strong heating localized at the shock (see the temperature panel in Fig. 2).

The magnetization parameter  $\sigma_{\text{bg}} \sim 25$  used in the simulation is far below its real value in a magnetar, and the shock strength should be scaled to a larger  $\sigma_{\text{bg}}$  according to Eq. (1). The corresponding large  $u^r \propto \sigma_{\text{bg}}$  will make the shock highly radiative, i.e. the accelerated flow will radiate its energy before crossing the shock and joining the downstream flow [19]. Future simulations could attempt to track radiative transfer with self-consistent creation of  $e^\pm$  pairs [48], which immediately make the flow optically thick. The dissipated energy is inevitably thermalized behind the shock, creating an opaque, radiation-dominated outflow. Our simulation assumes that the released energy remains trapped in the fluid. The observed relativistic outflow trails the shock, which expands with speed  $c$ .

*Black hole ring-down.* The ring-down of the nascent spinning black hole lasts  $\sim 100R_h/c$ . It involves quasi-periodic oscillations of the horizon with frequencies characteristic of

black hole quasi-normal modes, whose amplitude decays exponentially with time (e.g. [26]). For a stationary black hole, the quasi-monopolar magnetic flux  $\Psi$  threading the horizon would be stuck for a significant time — its decay would be controlled by magnetic reconnection in the equatorial plane on a timescale  $\gtrsim 100R_h/c$  [49]. By contrast, the oscillating black hole quickly and quasi-periodically sheds magnetic flux, losing significant  $\delta\Psi$  each oscillation period. The discharged  $\delta\Psi$  forms a quasi-periodic MHD outflow with the characteristic cusps of magnetic field lines in the equatorial plane. The cusps are inherited from the earlier split-monopole shape of field lines at the time of their decoupling from the oscillating black hole. This effect is seen in the simulation with the reduced rotation rate  $\nu = 56$  Hz (Fig. 1) and becomes stronger in the simulation with fast rotation  $\nu = 900$  Hz (Fig. 3).

Previous collapse simulations with a vacuum or FFE magnetosphere showed electromagnetic waves from ring-down [23–25, 50]. Vacuum ring-down is usually described as a coupling of black-hole quasi-normal modes to outgoing gravitational and electromagnetic waves [51, 52] using Newman-Penrose scalars

$$\psi_4 = -C_{\mu\nu\kappa\lambda} n^\mu \bar{m}^\nu n^\kappa \bar{m}^\lambda, \quad \phi_2 = F^{\mu\nu} \bar{m}_\mu n_\nu.$$

Here  $C_{\mu\nu\kappa\lambda}$  is the Weyl curvature tensor and  $F^{\mu\nu}$  is the electromagnetic tensor; vectors  $\mathbf{m}$  and  $\mathbf{n}$  are conveniently chosen as  $\mathbf{m} = (\hat{\theta} + i\hat{\phi})/\sqrt{2}$  and  $\mathbf{n} = (\hat{t} - \hat{r})/\sqrt{2}$  (so that  $\mathbf{m}$ ,  $\mathbf{n}$ , and  $\mathbf{l} = (\hat{t} + \hat{r})/\sqrt{2}$  form an orthonormal null tetrad). Then,



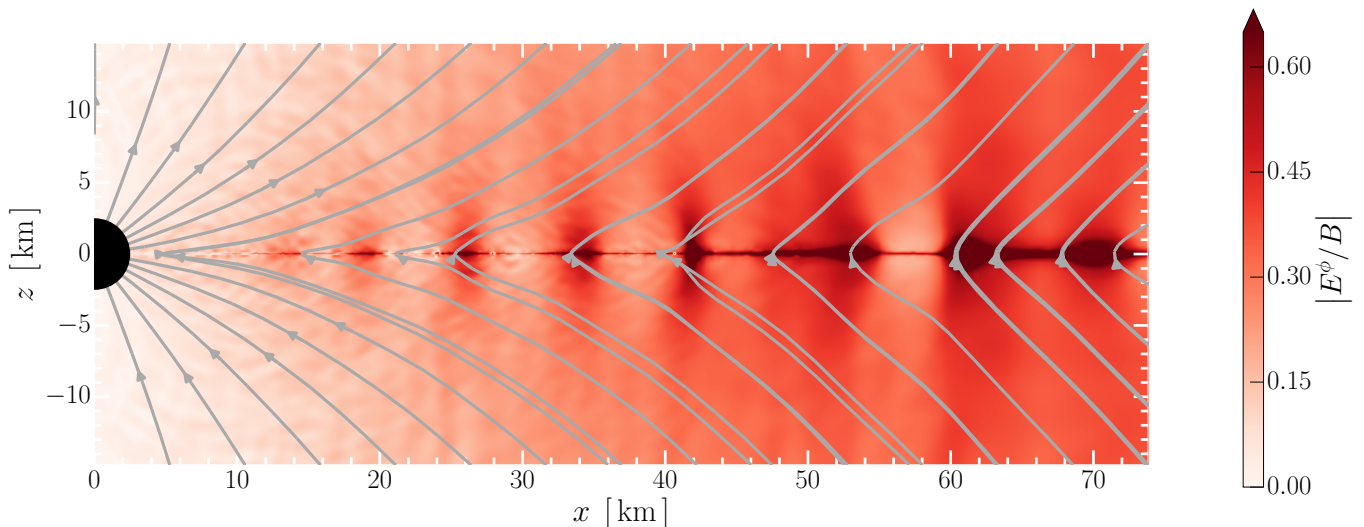


FIG. 3. Close-up of the black hole (black circle) and equatorial current sheet with magnetic field lines (gray) after the collapse of a neutron star with initial rotation  $\nu = 900$  Hz. Color shows the azimuthal component  $E^\phi$  of the electric field normalized to the magnetic field  $B$ . The snapshot is taken at time  $t = 0.67$  ms after the onset of collapse.

$\phi_2 \propto E_\theta + iE_\phi$  represents two polarization states of the outgoing electromagnetic waves (in MHD,  $E_\theta$  and  $E_\phi$  correspond to the fast magnetosonic and Alfvén waves, respectively). We have verified that the dominant (quadrupole) component of  $\psi_4$  observed in our simulation is consistent with the quasi-normal mode computed using `qnm` code [53]. We have also calculated the dominant (dipole) component of  $\phi_2$ , which also approximately matches the corresponding quasi-normal mode frequency (Fig. 4 shows the evolution of dominant spherical harmonics in  $\text{Im } \phi_2$  and  $\psi_4$ ). Note however that  $\phi_2$  was designed for vacuum electromagnetic fields, and so the oscillation of  $\phi_2$  may not accurately represent the modulation of MHD outflow. The frequency of compressive modulations observed in Fig. 3 may be directly estimated as  $\nu_{\text{mod}} = v/\lambda$ , where  $v \lesssim c$  is the outflow speed and  $\lambda \sim 7$  km is the spatial modulation period.

*Gamma-ray burst.* Our simulation demonstrates that the magnetospheric destruction during the neutron-star collapse involves strong dissipation and creates a powerful magnetized outflow with a characteristic duration  $\sim 1$  ms. The hot outflow is launched behind the leading monster shock and has a quasi-periodic tail. The modulated tail is generated by the nascent black hole, as it rings down and quickly sheds most of its magnetic flux initially inherited from the neutron star. The modulation frequency lies naturally in the kilohertz band, suggesting a connection with recently reported kilohertz quasi-periodic oscillations in some GRBs [54].

Note that the magnetosphere around the neutron star prior to collapse has a minute plasma density. Therefore, the explosion triggered by collapse is practically clean from baryons. The created  $e^\pm$  plasma in the hot outflow is initially opaque to scattering. Most of the heat density  $U$  is contained in trapped black body radiation  $U \approx aT^4$  ( $a$  is the radiation constant), as the photons far outnumber the  $e^\pm$  pairs. The outflow expan-

sion to large radii is not followed by our simulation, however its basic features can be predicted in analogy with the well-known “fireball” model for cosmological GRBs [55, 56]. The outflow Lorentz factor  $\gamma$  will grow and its temperature  $T$  will drop due to adiabatic cooling. Eventually, most of  $e^\pm$  pairs annihilate, and the trapped photons are released, producing a GRB. The burst duration is set by the outflow duration, which lasts only a few ms after the collapse.

The burst spectrum will peak at photon energies  $\sim 3k_B T \gamma$ , where  $k_B$  is the Boltzmann constant. Simplest GRB models assume adiabatic outflows with no magnetic fields, and then  $\gamma T \approx \text{const} = T_0$  [55]. In that case, the observed temperature is weakly changed during the outflow expansion and remains close to the initial temperature. Outflows predicted by our simulation are magnetically dominated, and their temperature may be affected by additional dissipation of magnetic energy at large radii. Regulation of the GRB spectral peak in dissipative outflows is discussed in [57].

The energy of the GRB outflow is set by the pre-collapse energy of the neutron-star magnetosphere  $\mathcal{E}_m \sim 10^{47} \mu_{33}^2$  erg. During the collapse the magnetospheric energy is amplified by compression, and then most of it is ejected in the outflow. Assuming that  $\sim 0.1$  of this energy is eventually emitted in the GRB, we can roughly estimate the GRB luminosity as  $L \sim 0.1 \mathcal{E}_m / 1 \text{ ms} \sim 10^{49} B_{15}^2$  erg/s, where  $B_{15} = B / 10^{15}$  G is the magnetic field near the neutron star prior to collapse. Note that the outflow (and hence the GRB) is anisotropic, but not strongly collimated.

During its lifetime prior to collapse, the rotating magnetar produced a magnetic wind outside the dipole magnetosphere. The collapse launches a relativistic shock, which will continue to expand into the cold wind. This leading shock is expected to emit a fast radio burst (FRB) at radii  $r \sim 10^{13}$  cm [8]. This suggests a mechanism for a delayed FRB from neutron star

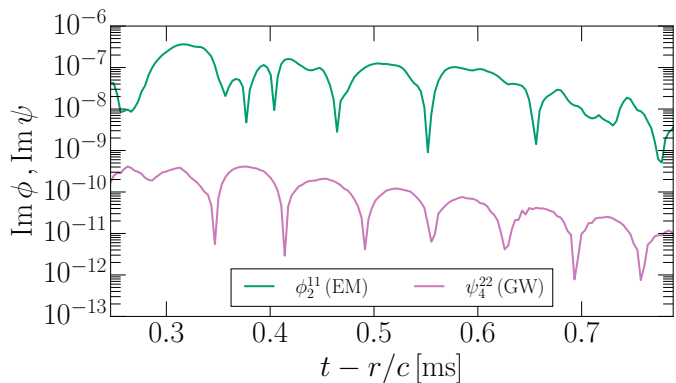


FIG. 4. Black hole ring-down of the rapidly rotating configuration,  $\nu = 900$  Hz. The ring-down in gravitational waves (GW) and in the electromagnetic field (EM) is shown using the Newman-Penrose scalars  $\psi_4$  ( $\ell = m = 2$  mode) and  $\phi_2$  ( $\ell = m = 1$  mode), respectively. All quantities are measured at a radius  $r \approx 75$  km.

mergers, emitted together with the delayed GRB. However, the FRB can hardly escape through the surrounding shell of mass  $M_{\text{ej}} \sim 10^{-2} M_{\odot}$  ejected earlier by the merger [58, 59]. A similar problem is faced by the recently proposed FRB-GRB connection [60].

The massive shell is also a treat to the GRB predicted by our simulation. The GRB will not be blocked by  $M_{\text{ej}}$  if the magnetar collapse occurs with a sufficient delay  $\Delta t \gtrsim 10$  hr after the merger, so that the massive ejecta expands to radius  $R \sim 3 \times 10^{14} (\Delta t/10 \text{ hr})$  cm and its optical depth to gamma-rays  $\tau \sim \kappa M_{\text{ej}}/4\pi R^2$  drops below unity ( $\kappa$  is the ejecta opacity to Compton scattering).

The authors gratefully acknowledge insightful discussions with A. Philippov, V. Ravi, R. Sari, L. Sironi, J. Stone, S. Teukolsky and C. Thompson. ERM acknowledges support by the National Science Foundation under grants No. PHY-2309210 and AST-2307394. A.M.B. is supported by NSF AST 2009453, NASA 21-ATP21-0056 and Simons Foundation award No. 446228. B.R. is supported by the Natural Sciences & Engineering Research Council of Canada (NSERC) and by a grant from the Simons Foundation (MP-SCMPS-00001470). Simulations were performed on the NSF Frontera supercomputer under grant AST21006, and on Delta at the National Center for Supercomputing Applications (NCSA) through allocation PHY210074 from the Advanced Cyberinfrastructure Coordination Ecosystem: Services & Support (ACCESS) program, which is supported by National Science Foundation grants #2138259, #2138286, #2138307, #2137603, and #2138296.

[1] P. Meszaros, Gamma-Ray Bursts, *Rept. Prog. Phys.* **69**, 2259 (2006), [arXiv:astro-ph/0605208](#).  
 [2] L.-X. Li and B. Paczynski, Transient events from neutron

star mergers, *Astrophys. J. Lett.* **507**, L59 (1998), [arXiv:astro-ph/9807272](#).  
 [3] B. D. Metzger, Kilonovae, *Living Rev. Rel.* **23**, 1 (2020), [arXiv:1910.01617 \[astro-ph.HE\]](#).  
 [4] B. P. Abbott *et al.* (LIGO Scientific, Virgo, Fermi-GBM, INTEGRAL), Gravitational Waves and Gamma-rays from a Binary Neutron Star Merger: GW170817 and GRB 170817A, *Astrophys. J. Lett.* **848**, L13 (2017), [arXiv:1710.05834 \[astro-ph.HE\]](#).  
 [5] A. Murguía-Berthier *et al.*, A Neutron Star Binary Merger Model for GW170817/GRB 170817A/SSS17a, *Astrophys. J. Lett.* **848**, L34 (2017), [arXiv:1710.05453 \[astro-ph.HE\]](#).  
 [6] O. Gottlieb, E. Nakar, T. Piran, and K. Hotokezaka, A cocoon shock breakout as the origin of the  $\gamma$ -ray emission in GW170817, *Mon. Not. Roy. Astron. Soc.* **479**, 588 (2018), [arXiv:1710.05896 \[astro-ph.HE\]](#).  
 [7] X. Xie, J. Zrake, and A. MacFadyen, Numerical Simulations of the Jet Dynamics and Synchrotron Radiation of Binary Neutron Star Merger Event GW170817/GRB 170817A, *Astrophys. J.* **863**, 58 (2018), [arXiv:1804.09345 \[astro-ph.HE\]](#).  
 [8] A. M. Beloborodov, Can a Strong Radio Burst Escape the Magnetosphere of a Magnetar?, *Astrophys. J. Lett.* **922**, L7 (2021), [arXiv:2108.07881 \[astro-ph.HE\]](#).  
 [9] L. Baiotti and L. Rezzolla, Binary neutron star mergers: a review of Einstein’s richest laboratory, *Rept. Prog. Phys.* **80**, 096901 (2017), [arXiv:1607.03540 \[gr-qc\]](#).  
 [10] D. Radice, S. Bernuzzi, and A. Perego, The Dynamics of Binary Neutron Star Mergers and GW170817, *Ann. Rev. Nucl. Part. Sci.* **70**, 95 (2020), [arXiv:2002.03863 \[astro-ph.HE\]](#).  
 [11] W. Kluzniak and M. Ruderman, The Central engine of gamma-ray bursters, *Astrophys. J. Lett.* **505**, L113 (1998), [arXiv:astro-ph/9712320](#).  
 [12] E. R. Most and E. Quataert, Flares, Jets, and Quasiperiodic Outbursts from Neutron Star Merger Remnants, *Astrophys. J. Lett.* **947**, L15 (2023), [arXiv:2303.08062 \[astro-ph.HE\]](#).  
 [13] L. Combi and D. M. Siegel, Jets from neutron-star merger remnants and massive blue kilonovae, (2023), [arXiv:2303.12284 \[astro-ph.HE\]](#).  
 [14] B. Giacomazzo and R. Perna, Formation of Stable Magnetars from Binary Neutron Star Mergers, *Astrophys. J. Lett.* **771**, L26 (2013), [arXiv:1306.1608 \[astro-ph.HE\]](#).  
 [15] B. Giacomazzo, J. Zrake, P. Duffell, A. I. MacFadyen, and R. Perna, Producing Magnetar Magnetic Fields in the Merger of Binary Neutron Stars, *Astrophys. J.* **809**, 39 (2015), [arXiv:1410.0013 \[astro-ph.HE\]](#).  
 [16] K. Kiuchi, P. Cerdá-Durán, K. Kyutoku, Y. Sekiguchi, and M. Shibata, Efficient magnetic-field amplification due to the Kelvin-Helmholtz instability in binary neutron star mergers, *Phys. Rev. D* **92**, 124034 (2015), [arXiv:1509.09205 \[astro-ph.HE\]](#).  
 [17] P. Mösta, D. Radice, R. Haas, E. Schnetter, and S. Bernuzzi, A magnetar engine for short GRBs and kilonovae, *Astrophys. J. Lett.* **901**, L37 (2020), [arXiv:2003.06043 \[astro-ph.HE\]](#).  
 [18] R. Aguilera-Miret, C. Palenzuela, F. Carrasco, and D. Viganò, The role of turbulence and winding in the development of large-scale, strong magnetic fields in long-lived remnants of binary neutron star mergers, (2023), [arXiv:2307.04837 \[astro-ph.HE\]](#).  
 [19] A. M. Beloborodov, Monster Radiative Shocks in the Perturbed Magnetospheres of Neutron Stars, *Astrophys. J.* **959**, 34 (2023), [arXiv:2210.13509 \[astro-ph.HE\]](#).  
 [20] P. D. Lasky, B. Haskell, V. Ravi, E. J. Howell, and D. M. Coward, Nuclear Equation of State from Observations of Short Gamma-Ray Burst Remnants, *Phys. Rev. D* **89**, 047302 (2014), [arXiv:1311.1352 \[astro-ph.HE\]](#).

- [21] V. Ravi and P. D. Lasky, The birth of black holes: neutron star collapse times, gamma-ray bursts and fast radio bursts, *Mon. Not. Roy. Astron. Soc.* **441**, 2433 (2014), arXiv:1403.6327 [astro-ph.HE].
- [22] S. Dall’Osso, B. Giacomazzo, R. Perna, and L. Stella, Gravitational waves from massive magnetars formed in binary neutron star mergers, *Astrophys. J.* **798**, 25 (2015), arXiv:1408.0013 [astro-ph.HE].
- [23] T. W. Baumgarte and S. L. Shapiro, Collapse of a magnetized star to a black hole, *Astrophys. J.* **585**, 930 (2003), arXiv:astro-ph/0211339.
- [24] L. Lehner, C. Palenzuela, S. L. Liebling, C. Thompson, and C. Hanna, Intense Electromagnetic Outbursts from Collapsing Hypermassive Neutron Stars, *Phys. Rev. D* **86**, 104035 (2012), arXiv:1112.2622 [astro-ph.HE].
- [25] E. R. Most, A. Nathanail, and L. Rezzolla, Electromagnetic emission from blitzars and its impact on non-repeating fast radio bursts, *Astrophys. J.* **864**, 117 (2018), arXiv:1801.05705 [astro-ph.HE].
- [26] K. D. Kokkotas and B. G. Schmidt, Quasinormal modes of stars and black holes, *Living Rev. Rel.* **2**, 2 (1999), arXiv:gr-qc/9909058.
- [27] N. Stergioulas and J. L. Friedman, Comparing models of rapidly rotating relativistic stars constructed by two numerical methods, *Astrophys. J.* **444**, 306 (1995), arXiv:astro-ph/9411032.
- [28] M. D. Duez, Y. T. Liu, S. L. Shapiro, and B. C. Stephens, Relativistic magnetohydrodynamics in dynamical spacetimes: Numerical methods and tests, *Phys. Rev. D* **72**, 024028 (2005), arXiv:astro-ph/0503420.
- [29] E. R. Most, L. J. Papenfort, and L. Rezzolla, Beyond second-order convergence in simulations of magnetized binary neutron stars with realistic microphysics, *Mon. Not. Roy. Astron. Soc.* **490**, 3588 (2019), arXiv:1907.10328 [astro-ph.HE].
- [30] Z. B. Etienne, V. Paschalidis, R. Haas, P. Mösta, and S. L. Shapiro, IllinoisGRMHD: An Open-Source, User-Friendly GRMHD Code for Dynamical Spacetimes, *Class. Quant. Grav.* **32**, 175009 (2015), arXiv:1501.07276 [astro-ph.HE].
- [31] F. Löffler *et al.*, The Einstein Toolkit: A Community Computational Infrastructure for Relativistic Astrophysics, *Class. Quant. Grav.* **29**, 115001 (2012), arXiv:1111.3344 [gr-qc].
- [32] D. Hilditch, S. Bernuzzi, M. Thierfelder, Z. Cao, W. Tichy, and B. Bruegmann, Compact binary evolutions with the Z4c formulation, *Phys. Rev. D* **88**, 084057 (2013), arXiv:1212.2901 [gr-qc].
- [33] M. Alcubierre, B. Bruegmann, P. Diener, M. Koppitz, D. Pollney, E. Seidel, and R. Takahashi, Gauge conditions for long term numerical black hole evolutions without excision, *Phys. Rev. D* **67**, 084023 (2003), arXiv:gr-qc/0206072.
- [34] L. Del Zanna, O. Zanotti, N. Bucciantini, and P. Londrillo, ECHO: an Eulerian Conservative High Order scheme for general relativistic magnetohydrodynamics and magnetodynamics, *Astron. Astrophys.* **473**, 11 (2007), arXiv:0704.3206 [astro-ph].
- [35] Z. B. Etienne, Y. T. Liu, and S. L. Shapiro, Relativistic magnetohydrodynamics in dynamical spacetimes: A new AMR implementation, *Phys. Rev. D* **82**, 084031 (2010), arXiv:1007.2848 [astro-ph.HE].
- [36] Z. B. Etienne, V. Paschalidis, Y. T. Liu, and S. L. Shapiro, Relativistic MHD in dynamical spacetimes: Improved EM gauge condition for AMR grids, *Phys. Rev. D* **85**, 024013 (2012), arXiv:1110.4633 [astro-ph.HE].
- [37] Y. T. Liu, S. L. Shapiro, Z. B. Etienne, and K. Taniguchi, General relativistic simulations of magnetized binary neutron star mergers, *Phys. Rev. D* **78**, 024012 (2008), arXiv:0803.4193 [astro-ph].
- [38] K. Kiuchi, K. Kyutoku, Y. Sekiguchi, M. Shibata, and T. Wada, High resolution numerical-relativity simulations for the merger of binary magnetized neutron stars, *Phys. Rev. D* **90**, 041502 (2014), arXiv:1407.2660 [astro-ph.HE].
- [39] C. Palenzuela, S. L. Liebling, D. Neilsen, L. Lehner, O. L. Caballero, E. O’Connor, and M. Anderson, Effects of the microphysical Equation of State in the mergers of magnetized Neutron Stars With Neutrino Cooling, *Phys. Rev. D* **92**, 044045 (2015), arXiv:1505.01607 [gr-qc].
- [40] R. Ciolfi, W. Kastaun, B. Giacomazzo, A. Endrizzi, D. M. Siegel, and R. Perna, General relativistic magnetohydrodynamic simulations of binary neutron star mergers forming a long-lived neutron star, *Phys. Rev. D* **95**, 063016 (2017), arXiv:1701.08738 [astro-ph.HE].
- [41] E. R. Most, Impact of a mean field dynamo on neutron star mergers leading to magnetar remnants, (2023), arXiv:2311.03333 [astro-ph.HE].
- [42] W. Kastaun, J. V. Kalinani, and R. Ciolfi, Robust Recovery of Primitive Variables in Relativistic Ideal Magnetohydrodynamics, *Phys. Rev. D* **103**, 023018 (2021), arXiv:2005.01821 [gr-qc].
- [43] J. V. Kalinani, R. Ciolfi, W. Kastaun, B. Giacomazzo, F. Cipolletta, and L. Ennoggi, Implementing a new recovery scheme for primitive variables in the general relativistic magnetohydrodynamic code Spritz, *Phys. Rev. D* **105**, 103031 (2022), arXiv:2107.10620 [astro-ph.HE].
- [44] S. M. Ressler, A. Tchekhovskoy, E. Quataert, and C. F. Gammie, The disc-jet symbiosis emerges: modelling the emission of Sagittarius A\* with electron thermodynamics, *Mon. Not. Roy. Astron. Soc.* **467**, 3604 (2017), arXiv:1611.09365 [astro-ph.HE].
- [45] E. R. Most, L. J. Papenfort, S. D. Tootle, and L. Rezzolla, On accretion discs formed in MHD simulations of black hole–neutron star mergers with accurate microphysics, *Mon. Not. Roy. Astron. Soc.* **506**, 3511 (2021), arXiv:2106.06391 [astro-ph.HE].
- [46] M. Chabanov, S. D. Tootle, E. R. Most, and L. Rezzolla, Crustal Magnetic Fields Do Not Lead to Large Magnetic-field Amplifications in Binary Neutron Star Mergers, *Astrophys. J. Lett.* **945**, L14 (2023), arXiv:2211.13661 [astro-ph.HE].
- [47] A. Y. Chen, Y. Yuan, X. Li, and J. F. Mahlmann, Propagation of a Strong Fast Magnetosonic Wave in the Magnetosphere of a Neutron Star, (2022), arXiv:2210.13506 [astro-ph.HE].
- [48] A. M. Beloborodov, Emission of Magnetar Bursts and Precursors of Neutron Star Mergers, *Astrophys. J.* **921**, 92 (2021), arXiv:2011.07310 [astro-ph.HE].
- [49] A. Bransgrove, B. Ripperda, and A. Philippov, Magnetic Hair and Reconnection in Black Hole Magnetospheres, *Phys. Rev. Lett.* **127**, 055101 (2021), arXiv:2109.14620 [astro-ph.HE].
- [50] C. Palenzuela, Modeling magnetized neutron stars using resistive MHD, *Mon. Not. Roy. Astron. Soc.* **431**, 1853 (2013), arXiv:1212.0130 [astro-ph.HE].
- [51] S. A. Teukolsky, Rotating black holes - separable wave equations for gravitational and electromagnetic perturbations, *Phys. Rev. Lett.* **29**, 1114 (1972).
- [52] S. A. Teukolsky, Perturbations of a rotating black hole. I. Fundamental equations for gravitational electromagnetic and neutrino field perturbations, *Astrophys. J.* **185**, 635 (1973).
- [53] L. C. Stein, qnm: A Python package for calculating Kerr quasinormal modes, separation constants, and spherical-spheroidal mixing coefficients, *J. Open Source Softw.* **4**, 1683 (2019), arXiv:1908.10377 [gr-qc].
- [54] C. Chirenti, S. Dichiara, A. Lien, M. C. Miller, and R. Preece,

- Kilohertz quasiperiodic oscillations in short gamma-ray bursts, *Nature* **613**, 253 (2023), [arXiv:2301.02864 \[astro-ph.HE\]](#).
- [55] B. Paczynski, Gamma-ray bursters at cosmological distances, *Astrophys. J. Lett.* **308**, L43 (1986).
- [56] J. Goodman, Are gamma-ray bursts optically thick?, *Astrophys. J. Lett.* **308**, L47 (1986).
- [57] A. M. Beloborodov, Regulation of the spectral peak in gamma-ray bursts, *Astrophys. J.* **764**, 157 (2013), [arXiv:1207.2707 \[astro-ph.HE\]](#).
- [58] M. Bhardwaj, A. Palmese, I. Magaña Hernandez, V. D’Emilio, and S. Morisaki, GW190425 and FRB20190425A: Challenges for Fast Radio Bursts as Multi-Messenger Sources from Binary Neutron Star Mergers, (2023), [arXiv:2306.00948 \[astro-ph.HE\]](#).
- [59] D. Radice, G. Ricigliano, M. Bhattacharya, A. Perego, F. J. Fattoyev, and K. Murase, What if GW190425 did not produce a black hole promptly?, (2023), [arXiv:2309.15195 \[astro-ph.HE\]](#).
- [60] A. Rowlinson, I. de Rutter, R. L. C. Starling, K. M. Rajwade, A. Hennessy, R. A. M. J. Wijers, G. E. Anderson, M. Mevius, D. Ruhe, K. Gourdji, A. J. van der Horst, S. ter Veen, and K. Wiersema, A coherent radio flash following a neutron star merger, *arXiv e-prints*, [arXiv:2312.04237 \(2023\)](#), [arXiv:2312.04237 \[astro-ph.HE\]](#).